Research Article | Vol. 24, No. 16 | 8 Aug 2016 | OPTICS EXPRESS 18297
Optics EXPRESS

Digital polarization holography advancing geometrical phase optics

LUCIANO DE SIO,[1,*] DAVID E. ROBERTS,[1] ZHI LIAO,[1] SARIK NERSISYAN,[1] OLENA USKOVA,[1] LLOYD WICKBOLDT,[1] NELSON TABIRYAN,[1] DIANE M. STEEVES,[2] AND BRIAN R. KIMBALL[2]

[1]*Beam Engineering for Advanced Measurements Co. (BEAM Co.), 1300 Lee Rd, Orlando, Florida 32810, USA*
[2]*US Army Natick Soldier Research, Development & Engineering Center, 15 General Greene Avenue, Natick, Massachusetts 01760, USA*
[*]*info@beamco.com*

Abstract: Geometrical phase or the fourth generation (4G) optics enables realization of optical components (lenses, prisms, gratings, spiral phase plates, etc.) by patterning the optical axis orientation in the plane of thin anisotropic films. Such components exhibit near 100% diffraction efficiency over a broadband of wavelengths. The films are obtained by coating liquid crystalline (LC) materials over substrates with patterned alignment conditions. Photo-anisotropic materials are used for producing desired alignment conditions at the substrate surface. We present and discuss here an opportunity of producing the widest variety of "free-form" 4G optical components with arbitrary spatial patterns of the optical anisotropy axis orientation with the aid of a digital spatial light polarization converter (DSLPC). The DSLPC is based on a reflective, high resolution spatial light modulator (SLM) combined with an "ad hoc" optical setup. The most attractive feature of the use of a DSLPC for photoalignment of nanometer thin photo-anisotropic coatings is that the orientation of the alignment layer, and therefore of the fabricated LC or LC polymer (LCP) components can be specified on a pixel-by-pixel basis with high spatial resolution. By varying the optical magnification or de-magnification the spatial resolution of the photoaligned layer can be adjusted to an optimum for each application. With a simple "click" it is possible to record different optical components as well as arbitrary patterns ranging from lenses to invisible labels and other transparent labels that reveal different images depending on the side from which they are viewed.

©2016 Optical Society of America

OCIS codes: (090.1995) Digital holography; (240.5440) Polarization-selective devices; (260.1440) Birefringence; (160.3710) Liquid crystals.

References and links

1. T. Scharf, *Polarized Light in Liquid Crystals and Polymers* (John Wiley and Sons, 2006).
2. C. S. Wu and S. T. Wu, "Liquid-crystal-based switchable polarizers for sensor protection," Appl. Opt. **34**(31), 7221–7227 (1995).
3. M. D. Lavrentovich, T. A. Sergan, and J. R. Kelly, "Switchable broadband achromatic half-wave plate with nematic liquid crystals," Opt. Lett. **29**(12), 1411–1413 (2004).
4. S. R. Nersisyan and N. V. Tabiryan, "Polarization imaging components based on patterned photoalignment," Mol. Cryst. Liq. Cryst. (Phila. Pa.) **489**(1), 156–168 (2008).
5. R. Magnusson and T. K. Gaylord, "Diffraction efficiencies of thin phase gratings with arbitrary grating shape," J. Opt. Soc. Am. **68**(6), 806–809 (1978).
6. M. G. Moharam and T. K. Gaylord, "Rigorous coupled-wave analysis of planar-grating diffraction," J. Opt. Soc. Am. **71**(7), 811–818 (1981).
7. L. De Sio, N. Tabiryan, T. Bunning, B. R. Kimball, and C. Umeton, "Dynamic Photonic Materials based on Liquid Crystals," Prog. Opt. **58**, 1–64 (2013).
8. B. Bahadur, *Liquid Crystals – Applications and Uses* (World Scientific, 1990).
9. K. H. Kim and J. K. Song, "Technical evolution of liquid crystal displays," NPG Asia Mater. **1**(1), 29–36 (2009).
10. S. R. Nersisyan, N. V. Tabiryan, D. M. Steeves, and B. R. Kimball, "The Promise of Diffractive Waveplates," Opt. Photonics News **21**(3), 40–45 (2010).
11. N. Tabiryan, D. Roberts, E. Serabyn, D. Steeves, and B. Kimball, "Superlens in the skies: liquid-crystal-polymer technology for telescopes," SPIE Newsroom, http://spie.org/newsroom/6317-superlens-in-the-skies-liquid-crystal-polymer-technology-for-telescopes?ArticleID=x117044 (2016).

#268114 http://dx.doi.org/10.1364/OE.24.018309
Journal © 2016 Received 13 Jun 2016; revised 24 Jul 2016; accepted 25 Jul 2016; published 1 Aug 2016

Optics EXPRESS

12. Z. Bomzon, G. Biener, V. Kleiner, and E. Hasman, "Space-variant Pancharatnam-Berry phase optical elements with computer-generated subwavelength gratings," Opt. Lett. **27**(13), 1141–1143 (2002).
13. L. Marrucci, C. Manzo, and D. Paparo, "Pancharatnam-Berry phase optical elements for wave front shaping in the visible domain: switchable helical mode generation," Appl. Phys. Lett. **88**(22), 221102 (2006).
14. S. R. Nersisyan, N. V. Tabiryan, D. M. Steeves, and B. R. Kimball, "Optical axis gratings in liquid crystals and their use for polarization insensitive optical switching," J. Nonlinear Opt. Phys. Mater. **18**(01), 1–47 (2009).
15. S. R. Nersisyan, N. V. Tabiryan, L. Hoke, D. M. Steeves, and B. R. Kimball, "Polarization insensitive imaging through polarization gratings," Opt. Express **17**(3), 1817–1830 (2009).
16. N. V. Tabiryan, S. R. Nersisyan, H. Xianyu, and E. Serabyn, "Fabricating vector vortex waveplates for coronagraphy," IEEE Aerospace Conference, 1–12, 2012.
17. N. V. Tabiryan, S. V. Serak, S. R. Nersisyan, D. E. Roberts, B. Ya. Zeldovich, D. M. Steeves, and B. R. Kimball, "Broadband waveplate lenses," Opt. Express **24**(7), 7091–7102 (2016).
18. N. V. Tabiryan, S. V. Serak, D. E. Roberts, D. M. Steeves, and B. R. Kimball, "Thin waveplate lenses of switchable focal length--new generation in optics," Opt. Express **23**(20), 25783–25794 (2015).
19. K. Gao, H. H. Cheng, A. Bhowmik, C. McGinty, and P. Bos, "Nonmechanical zoom lens based on the Pancharatnam phase effect," Appl. Opt. **55**(5), 1145–1150 (2016).
20. L. Nikolova and P. S. Ramanujam, *Polarization holography* (Cambridge, 2009).
21. G. P. Crawford, J. N. Eakin, M. D. Radcliffe, A. Callan-Jones, and R. A. Pelcovits, "Liquid-crystal diffraction gratings using polarization holography alignment techniques," J. Appl. Phys. **98**(12), 123102 (2005).
22. A. Mazzulla, A. Dastoli, G. Russo, L. Lucchetti, and G. Cipparrone, "Polarization holographic techniques: a method to produce diffractive devices in polymer dispersed liquid crystals," Liq. Cryst. **30**(1), 87–92 (2003).
23. A. G. Poleshchuk, E. G. Churin, V. P. Koronkevich, V. P. Korolkov, A. A. Kharissov, V. V. Cherkashin, V. P. Kiryanov, A. V. Kiryanov, S. A. Kokarev, and A. G. Verhoglyad, "Polar coordinate laser pattern generator for fabrication of diffractive optical elements with arbitrary structure," Appl. Opt. **38**(8), 1295–1301 (1999).
24. C. Ye, "Construction of an optical rotator using quarter-wave plates and an optical retarder," Opt. Eng. **34**(10), 3031–3035 (1995).
25. V. Bagini, R. Borghi, F. Gori, M. Santarsiero, F. Frezza, G. Schettini, and G. Spagnolo, "The Simon–Mukunda polarization gadget," Eur. J. Phys. **17**(5), 279–284 (1996).
26. http://www.axometrics.com/6.htm.
27. F. Moia, H. Seiberle, and M. Schadt, "Optical LPP/LCP devices: a new generation of optical security elements," Proc. SPIE **3973**, 196–203 (2000).
28. C. Carrasco-Vela, X. Quintana, E. Otón, M. A. Geday, and J. M. Otón, "Security devices based on liquid crystals doped with a colour dye," Opto-Electron. Rev. **19**(4), 496–500 (2011).

1. Introduction

Polarization control of electromagnetic radiation can be obtained by utilizing conventional optical elements - polarizers. These are capable of converting an unpolarised light into linear (or circular) polarized state through a separation of orthogonal electric field components, one of which is subsequently absorbed, deflected, or reflected. A waveplate (WP) or a phase retarder is used to affect the polarization state of a light wave propagating through it. WPs are manufactured with birefringent materials (such as quartz, mica, or a liquid crystal polymer) for which the refractive index depends on the angles between the anisotropy axes and the electric field of the light wave. The retardation introduced by a WP depends on the thickness of the birefringent material, the wavelength of the light, and the refractive indices along the axes of the material. By selecting the relationship between these parameters, it is possible to introduce a controlled phase shift between the two polarization components of a light wave, thereby altering its polarization [1]. Switchable polarization control optical elements (polarizers or WPs) based on liquid crystal (LC) materials are critical in the development of photonic devices [2–4]. Indeed, optics has been evolving by developing components with different characteristics due to modulation of: shape or thickness (first generation, 1G Optics) [5]; the refractive index (second generation, 2G Optics) [6,7]; and the magnitude of the optical anisotropy (third generation, 3G Optics) [8,9]. The new, fourth generation optical components (geometrical phase or 4G Optics) are, in essence, diffractive WPs (DWs) made of thin anisotropic polymer films comprising, in particular, LC molecules in their structure [10–13]. The specific function of these components is obtained by modulating the orientation of the anisotropy axis in the plane of the waveplate. A linear variation of the orientation of the anisotropy axis in the plane of the waveplate results in a prism-like action [14,15]. These components are often referred to as cycloidal diffractive waveplates due to the pattern characterizing the spatial distribution of the anisotropy axis. The variation of the orientation angle around an axis perpendicular to the plane of the waveplate yields the equivalent of a

Optics EXPRESS

spiral waveplate, often referred to as a vector vortex waveplate [16]. By varying the angle proportional to the square of the distance from the axis (parabolic variation), it is possible to obtain a lens [17–19]. Fabrication of 4G optical components presents many challenges. The principal techniques for patterning light polarization include polarization holography [20–22] and laser direct-writing [23] scanning. Polarization holography enables realization of 4G optical components with spatial symmetry including polarization gratings and lenses. However, every single component requires a different optical setup with its own complexity. The same methodology can be used for realizing arbitrary wavefronts by combining an interferometric technique and a physical object. The second fabrication method (direct-write laser scanning), involves directly recording a wavefront by continuously scanning a well focused laser beam. The technique is powerful but, at the same time, is quite cumbersome since it requires three degrees of freedom (two for the spatial scanning and one for controlling the anisotropic orientation). Also, mechanically moving systems complicate the setup. Arbitrary spatially varying geometrical phase elements have not been well exploited so far due to the lack of fabrication techniques. The DSLPC represents a very important step-forward with respect to the previously reported techniques. In fact, it not only enables the realization of optical components with spatial symmetry (e.g. lenses, gratings, etc..) by means of the same optical setup but, it allows the realization of any kind arbitrary wavefront. Moreover, the DSLPC technique is straightforward since with a simple "click", different kinds of optical structures (lens arrays, vortex arrays and gratings) and arbitrary photoalignment patterns can be recorded in few nanometer thick photoanisotropic material. Furthermore, the DSLPC does not utilize any mechanical movement (like the direct-write laser scanning) and it is not affected by mechanical vibrations (like the polarized interference lithography) since it is a single beam recording process. In this paper, we report a generalized approach for realizing DWs with arbitrary modulation of the optical axis orientation, based on DSLPC. The new methodology allows realization of any kind of "free-form" optical components with any desired parameter (e.g. focal length, periodicity, topological charge, etc.) as well as elements including arbitrary and complex patterns.

2. Optical setup

The optical layout used for the demonstration of the working principle of the DSLPC is shown in Fig. 1. A linearly-polarized laser beam (λ = 532nm, frequency-doubled Nd:YAG laser) is spatially filtered (through the lens L1 and the aperture A) prior to collimation (through the lens L2). The linear polarizer P1 improves the polarization quality of the collimated beam, which is then converted to a circular polarized one by a quarter wave plate (QWP1) in the appropriate orientation (45°) with respect to the polarization axis of the input beam. The propagating beam is reflected/diffracted by a reflective, high resolution (pixel size 6.4μm) phase only spatial light modulator (SLM) (see section 3.1 for more information). The highly diffracted 0th order (reflection efficiency 78%) is converted into a linear polarized beam by means of a second QWP2 (its axis is set at - 45° with respect to the polarization direction of the input laser beam). The birefringent medium (LC) produces a spatially modulated phase offset between the linear polarized components of the incident beam, and this phase offset pattern is converted into spatial modulation of the direction of linear polarization after QWP2. The phase retardation is programmable from pixel to pixel (see inset of Fig. 1) by varying the input grayscale level or digital number (DN) (different grayscale levels translate into different driving voltages applied to each pixel of the LC SLM). Mathematical analyses are available in the literature [24,25] that demonstrate this effect for a basic version of the optical system shown in Fig. 1.

Optics EXPRESS

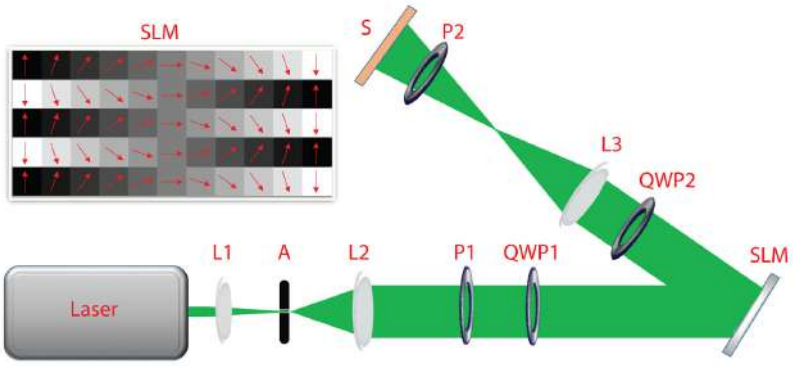

Fig. 1. Sketch of the DSLPC optical setup. L1, L2, L3, lenses; A, aperture; P1, P2, polarizers; QWP1, QWP2, quarter waveplates; SLM, spatial light modulator; S, sample coated with photoanisotropic material. Photo-insert shows the schematic of the digital control (pixel to pixel) of light polarization.

The lens L3 in the setup is used to image the light reflected by the SLM onto the substrate (S) carrying the photoanisotropic coating such as there is a one-to-one spatial correspondence between the phase retardation introduced by the SLM and the optical axis orientation in the generated pattern. The projected image on the sample can be larger than the SLM area (i.e. magnified), smaller than the SLM area (i.e. de-magnified), or the same size as the SLM (i.e. imaged one-to-one), depending on application requirements. The polarizer P2 is removed in the recording process.

3. Materials and methods

3.1 Spatial light modulator

The SLM (LETO, Holoeye, liquid crystal on silicon technology, LCOS) is addressed via a standard DVI signal by a PC's graphics card. Basically the LCOS display works like an extended monitor, where all the phase functions (e.g. lens, grating, holograms, etc…) are addressed via DVI. The SLM is a LC based birefringent medium made of an array of pixels (1920*1080) with an active area of 12.5 x 7.1 mm which can be addressed with 256 grey levels (named digital numbers, DN) and a fill factor of about 93%.

3.2 Photo-alignment material

The PAL layer (PAAD-72, BEAM Co.) is an azobenzene based material dissolved in an organic solvent (Dimethylformamide, DMF) and possesses a broad absorption band extended to visible part of the spectrum, Fig. 2.

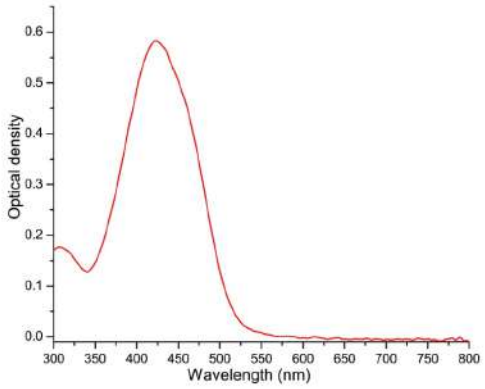

Fig. 2. Absorbance spectrum of a 1 wt.% solution of PAAD-72 in DMF with 10 µm cell thickness.

Optics EXPRESS

Thus, PAAD-72 allows photoalignement with laser light in the blue or green regions of the spectrum. PAL was spin-coated onto substrates at 3000 rpm for 30 s. The thickness of the PAAD layer used for photoalignment is of the order of 10 nm.

3.3 Liquid crystal monomer

The liquid crystal monomer solution RLCS-7 (BEAM Co.) was deposited on the PAL layer after recording each specific DW component. The DW fabrication process is shown in Fig. 3.

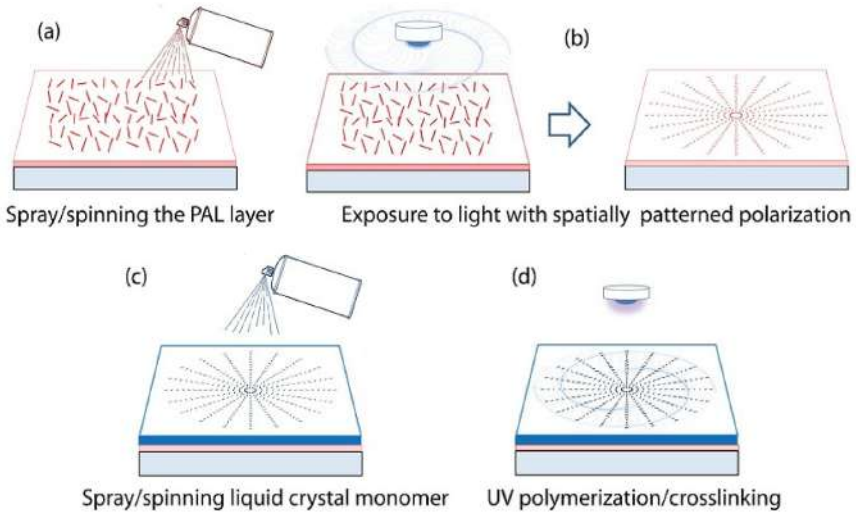

Fig. 3. Sketch of the fabrication process of a liquid crystal polymer DW component.

After PAL deposition [Fig. 3(a)], the substrate is exposed to the DSLCP pattern [Fig. 3(b)] where the specific polarization orientation is recorded. Subsequently, the substrate is covered with the liquid crystal monomer [Fig. 3(c)]. The rotation speed is adjusted so that the thickness of the final polymer layer would induce half wave of retardation at a wavelength of 532 nm. In this way, we produced a DW optimized for a wavelength of 532 nm by spin-coating a single layer of liquid crystal monomer at a rotational speed of 3000 rpm on the PAL layer. Time of spin-coating was 1 minute and the liquid crystal monomer was cured with unpolarised UV light at 365 nm wavelength and an intensity of 15 mW/cm^2 with an exposure time of 5 minutes [Fig. 3(d)].

3.4 Mathematical analysis of the phase masks

For an optical axis orientation α, the digital number (DN) sent to the SLM is DN = 255*frac(α/π), where frac(α/π) is the fractional part of real number α/π. For Figs. 4(a) and 4(e), optical axis orientation angle varies as $\alpha = \pi r^2/2\lambda F$ where r is the distance from the nearest center of a lenslet and F is the focal length of the lenslet at wavelength λ [20,21]. For Fig. 4i (Axicon) the optical axis orientation angle is $\alpha = \pi \cdot (r/r_0)$ where r is the distance from the center of the SLM and r_0 = 100 μm. For Fig. 4(o), the optical axis orientation $\alpha(x, y)$ at any point described by transverse Cartesian coordinates (x, y) is defined as follows: optical axis pattern defined over an area of $0 \le x \le 12.3$ mm, $0 \le y \le 6.9$ mm, n_x = floor(x/L), n_y = floor(y/L). Azimuthal angle φ = atan2[(y - n_yL), (x - n_xL)], q = order or degree of the vector vortex array, an integer or half-integer (q = ½ as an example). For n_x and n_y both even, $\alpha(x, y) = q\varphi$. For n_x even and n_y odd, $\alpha(x, y) = -q\varphi$. For n_x odd and n_y even, $\alpha(x, y) = q(\pi - \varphi)$. For n_x and n_y both odd, $\alpha(x, y) = -q(\pi - \varphi)$. Here floor($b$) is the largest integer smaller than positive real number b, and atan2(y, x) is the two-argument arc tangent function, satisfying $-\pi < \text{atan2}(y, x) \le \pi$.

Optics EXPRESS

3.5 Dichroic dye doped polymerizable liquid crystal

The material composition was prepared by mixing an LC acrylate monomer PLC-20-14C (BEAM Co) with a 2 wt.% of photoinitiator (Darocur-4265 from Ciba) and 1 wt.% of zeolite LCs. The gap of the cell was filled with the dichroic dye doped polymerizable LC mixture by capillary action in darkness above the clearing temperature (85°C) ensuring complete transition to the isotropic state of the light sensitive LC. The samples were slowly cooled (2 K/min) to room temperature before photopolymerization (20 min, 3 mW/cm^2 at 420 nm).

4. Experimental results

As a proof of concept, in order to show the extraordinary versatility of the DSLCP, we have selected for illustration four phase masks corresponding to different optical elements such as a fast diffractive microlens array, a slow diffractive microlens array, an axicon and a vortex array. The polarization patterns generated by the DSLCP system were recorded on a glass substrate (typically BK7 glass) coated with a photoalignment layer (PAL, see section 3.2 for more information) with 20 min exposure time to a beam of 6 mW/cm^2 power density. After recording the photoalignment pattern for each DW, a layer of LC monomer solution was spin-coated over the PAL layer (see section 3.3 for more information).

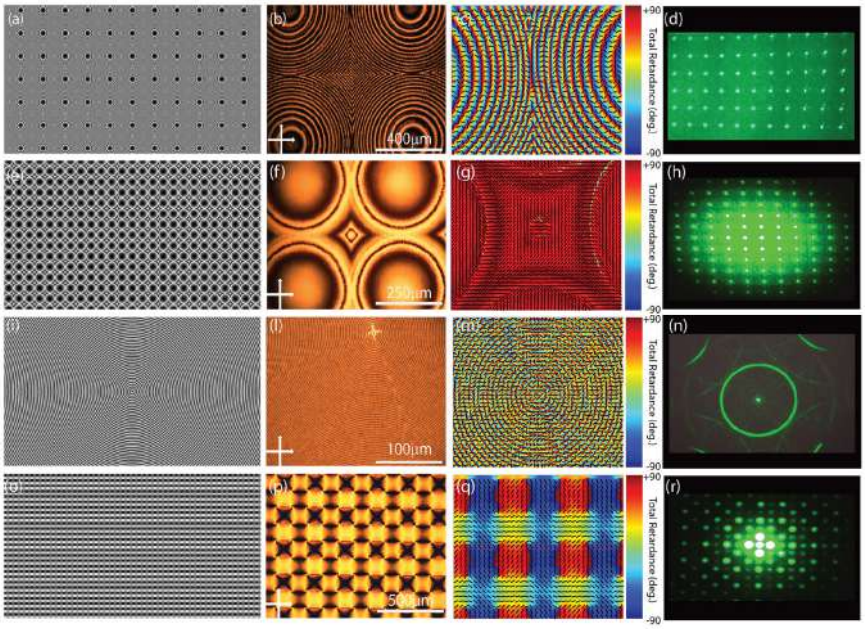

Fig. 4. Phase mask input to SLM of a fast (a), slow (e), diffractive lenslet arrays along with the POM view of the product sample (b), (f) and their corresponding Mueller matrix polarimeter characterization (c), (g). Phase mask of an axicon (i), a vortex array (o) along with the POM view of the samples (l), (p) and their corresponding Mueller matrix polarimeter characterization (m), (q). Images (d), (h), (n), (r) are the corresponding far field diffraction patterns.

Figure 4(a) represents the phase masks of a short focal length lenslet array. Figure 4(b) is the polarized optical microscope (POM) views of the component highlighting the continuous boundary conditions between neighbouring lenslets. The molecular axis orientation was characterized by a Mueller Matrix Spectroscopic Polarimeter [26]. It demonstrates that the optical axis continuously rotates from the center of one lenslet to another over an angular range of approximately 180° [Fig. 4(c)]. The distance between the centers of adjacent square lenslets is 1.07 mm. The focal length of each lenslet at a wavelength of λ = 532 nm is 30 mm. Figure 4(e) represents the phase masks of a long focal length lenslet array. The series of images of Figs. 4 (e)-4(g) shows the progression from the mathematical model [Fig. 4(e)] to

Optics EXPRESS

the POM view of the sample [Fig. 4(f)], to the optical axis modulation pattern to the resulting lenslet array acquired with the imaging spectropolarimeter [Fig. 4(g)]. It shows a continuous rotation of the molecular axis orientation of about 140°. The distance between the centers of adjacent square lenslets is 494 μm. The focal length of each lenslet at 532 nm wavelength is 57 mm. Figure 4(i) is a phase mask of an Axicon, with an optical axis periodic along the radial coordinate. Figure 4(l) shows the POM view of the sample having the periodicity along the radial coordinate with a modulation of the optical axis orientation of about 180° [Fig. 4(m)]. Lastly, Fig. 4(o) shows the phase mask of a vector vortex array with continuous boundaries between cells of the array. Each cell of the array is a square with side length L = 128 μm. The POM view of the sample highlighting a cell-like structure is displayed in Fig. 4(p) while its spectropolarimeter image reported in Fig. 4(q) shows a continuous rotation of the optical axis orientation across the cells of the array of about 180°. Noteworthy, the vector vortex array [Fig. 4(o)] can be used for realizing a breakthrough in the telecommunication field by multiplexing/demultiplexing through the topological charge the data stream. Figures 4(d) –4(h)- 4(n)-4 (r) are the far field diffraction patterns obtained by probing the DWs (reported in Figs. 4 (b)-4(f)-4(l)-4(p), respectively) with a linearly polarized laser beam (λ = 532 nm). For more details on the mathematical modelling of the used phase masks see section 3.4.

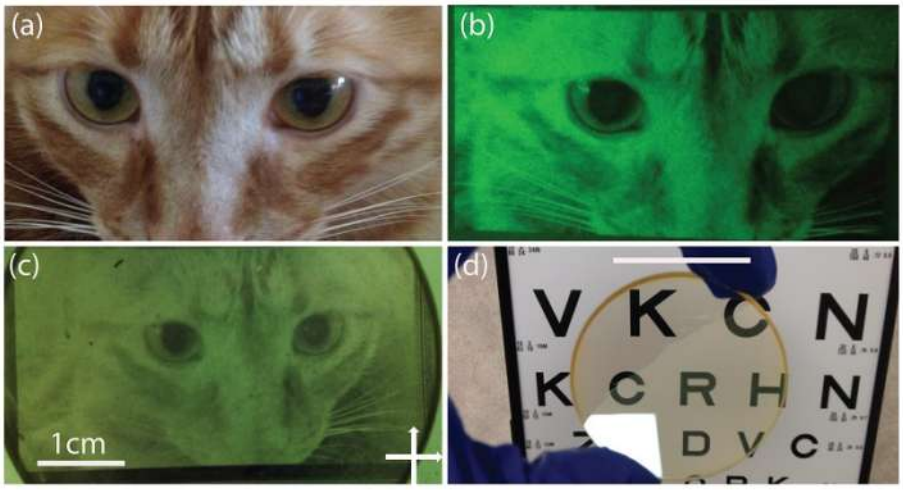

Fig. 5. Photo of a cat transformed into a phase mask input to SLM (a) along with the generated polarization pattern (b) after passing the light through a linear polarizer. POM view of the DW (c). View of the eye acuity chart through the "invisible" cat (d).

So far we have demonstrated that the DSLCP technique can be used for recording DWs with periodic modulation of the optical axis orientation. The DSLCP can be employed for making DWs with arbitrary orientation of the optical axis orientation, acting as a powerful tool for realizing invisible DWs. In order to show the concept, we have sent as an input to the SLM a photo of a cat [Fig. 5(a)]. Figure 5(b) is the generated polarization pattern through the DSLCP visualized by means of a polarizer (Fig. 1, P2) while it is totally invisible without the polarizer as shown in Visualization 1. Figure 5(c) shows a POM view of the recorded DW component while it appears transparent in unpolarised light, as illustrated in Fig. 5(d) (invisible cat). Another example of DW with arbitrary orientation of the optical axis orientation with applications ranging from security to anti-counterfeiting is the invisible barcode shown in Fig. 6.

Optics EXPRESS

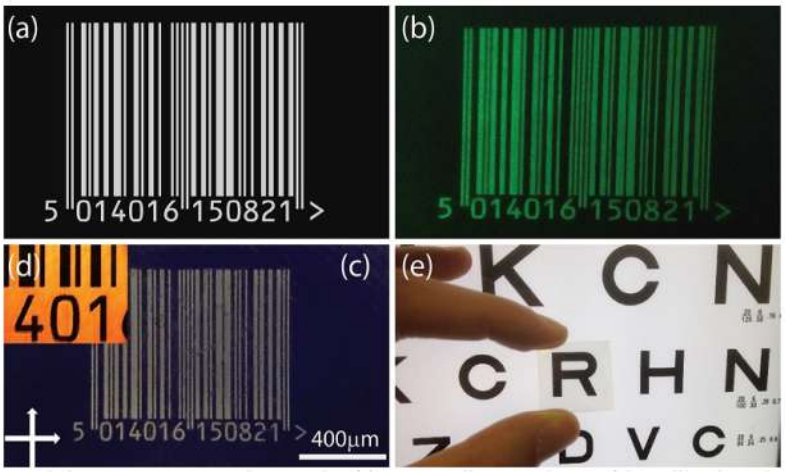

Fig. 6. Phase mask input to SLM (a); photograph of image at alignment layer of laser-illuminated SLM, viewed through polarization analyser (b); POM view of the DW barcode along with a photomicrograph of a section of the DW bar code made with phase mask (a); view of eye acuity chart through LCP with the invisible barcode image (e).

Figure 6(a) displays the input mask sent to the SLM display. Figure 6(b) is the generated polarization pattern through the DSLCP visualized by means of a polarizer (Fig. 1, P2) meanwhile turns to be totally invisible without it (see Visualization 2). Figures. 6(c) and 6(d) are a POM photo and micrograph of the realized DW barcode, respectively. The component is totally transparent in unpolarised light, as illustrated in Fig. 6(e).

Fig. 7. Photo of George Washington used as a phase mask input to SLM (a) along with the generated polarization pattern after passing the light through a linear polarizer (b). POM view of the product DW (c). Photo of the United States passport (specimen) after transferring the translucent DW film encoding the George Washington photo without (d) and with the polarizer/analyser (e).

Optics EXPRESS

The fact that DWs appear completely transparent in natural unpolarized light [Fig. 5(d) and Fig. 6(e)] suggests applications such as security features wherein information is encoded in an apparently transparent layer or coating [27]. This opens the opportunity of developing novel security and authentication system to be applied in variety of documents, credit cards, and other products. To this purpose, we have used as phase mask the George Washington picture [Fig. 7(a)] which is nowadays used in the United States one-dollar bill. Figure 7(b) is the generated polarization pattern through the DSLCP and visualized by means of a polarizer (Fig. 1, P2). Figure 7(c) is the recorded DW component which has been released from its own substrate and transferred to the United States passport (specimen) after making an opening with oval shape [Fig. 7(d)]. The information could then be revealed [Fig. 7(e)] when the layer was observed with an appropriate polarization-sensitive viewing system, which may be as simple as the polarized glasses used in 3D cinema (see Visualization 3).

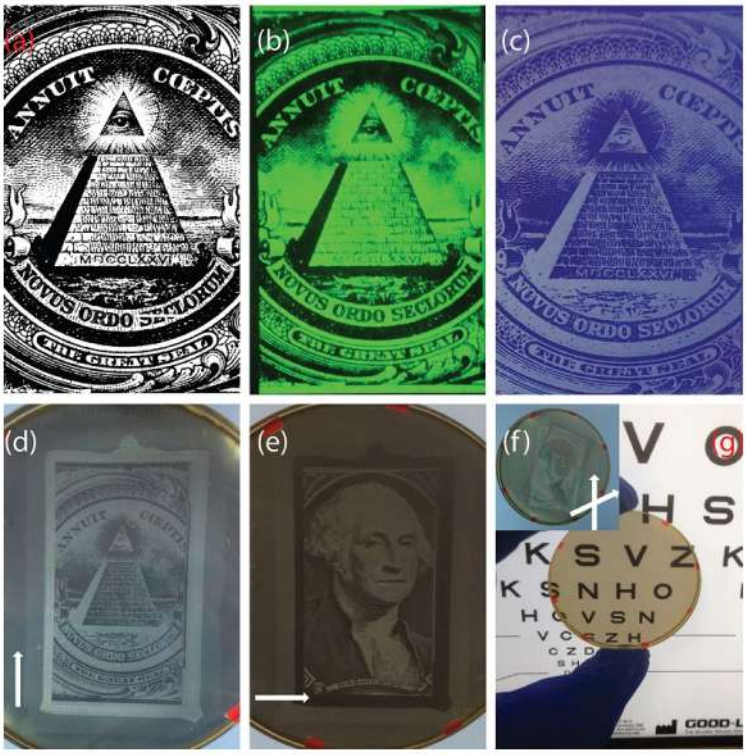

Fig. 8. Photo of the Great Pyramid used as a phase mask input to SLM (a) along with the generated polarization pattern after passing the light through a linear polarizer (b) and the resultant DW (c). Dual side label showing from one side the pyramid (d) and from the other side the George Washington picture (e). View of the eye acuity chart through the invisible dual label (g) along with the POM image showing both images (f).

Figure 8(a) (the Great Pyramid image) shows another example of a DW film with arbitrary orientation of the optical axis orientation pattern while Fig. 8(b) is the corresponding polarization pattern through the DSLCP and visualized by means of a polarizer (Fig. 1, P2). The corresponding DW component is shown in Fig. 8(c). Another very interesting opportunity as a security feature is based on the possibility to generate an invisible dual-sided label where by applying different alignment conditions and different images on the opposing glass substrates makes it possible to create different latent images on each side of one single device. For a demonstration, we have patterned two glass substrates, one with the Great Pyramid image [Fig. 8(a)] and another one with the George Washington picture [Fig. 7(a)]. The two substrates were brought into contact via 50 μm spacers and filled with a dichroic dye doped room-temperature polymerizable LC (see section 3.5 for more details). The working

principle of the device (described in details in [28]) is based on the ability of a dichroic dye oriented by the polymerizable LC to absorb light parallel to the direction of its long axis. During the photo-patterning of the two images there are different orientation directions which identify the areas that will eventually appear clear or dark when polarized light impinges the device. Figure 8(d) shows one of the two images (the Great Pyramid) visible from one side when the incident light is vertical aligned while Fig. 8(e) displays the second image (the George Washington picture) obtained by flipping the sample for light horizontally polarized. If no polarizer is used, no image is visible but a homogeneous color corresponding to the dichroic dye used [Fig. 8(g)]. Instead, both images are clearly visible if the substrate is placed between crossed polarizers [Fig. 8(f)]. Rotating the analyzer, individual pictures or their negatives can be selected.

4. Conclusion

To summarize, we have described a digital method for controlling the polarization of a light source, enabling the realization of a new generation of optical components with arbitrary modulation of the optical axis orientation. We have exploited the universal capability of a digital spatial light polarization converter (DSLPC) made by combining a high resolution spatial light modulator (SLM) and a single beam optical recording setup. Using the DSLPC setup, with a simple "click", different kinds of "free-form" optical structures (lens array, grating and a vortex array) have been recorded in few micron thick liquid crystal polymer as well as liquid crystal layers to allow switching the images on and off. The technique allows realization of invisible labels which are completely transparent in natural unpolarised light enabling a new methodology for realizing new security and authentication systems to be applied as anti-counterfeiting features. As an example, we have applied the invisible label technology to the United States passport (specimen) by transferring the diffractive waveplate layer encoding the George Washington photo. Further improvement, as a security feature, has been obtained by realizing an invisible dual-sided label where two latent images (one for each side) can be seen. The technique represents a digital breakthrough in the field of 4G Optics where, actually, the only limitation is dictated by human imagination.

Funding

This work was supported by the US Army Natick Soldier Research, Development and Engineering Center (NSRDEC).

Acknowledgments

We thank U. Hrozhyk, J. Hwang, H. Xianyu and R. Vergara for discussions and assistance.